

# A Biophysical model of bidirectional synaptic plasticity: dependence on AMPA and NMDA receptors

Gastone C. Castellani<sup>1</sup>, Elizabeth M. Quinlan<sup>2</sup>, Leon N Cooper<sup>3,4,5</sup> and Harel Z. Shouval<sup>3,†</sup>

<sup>1</sup>Physics Department, CIG and Dimorfipa Bologna University, Bologna 40121, Italy and <sup>2</sup> Department of Biology, University of Maryland, College Park, MD 20742 <sup>3</sup>Institute for Brain and Neural Systems, <sup>4</sup>Department of Neuroscience and <sup>5</sup>Department of Physics Brown University, Providence, RI 02912

† Corresponding Author Institute for Brain and Neural Systems Box 1843 Brown University Providence RI, 02912 Email: hzs@cns.brown.edu Phone: 401-863-2187 Fax: 401-863-3494

## Characters, figures etc.

Abstract: 224 Words

Characters: 30000

Figures-4:

figure 1: 1 column X 6cm= $180 \times 6 = 1080$

figure 2: 1 column X 12cm= $180 \times 12 = 2160$

figure 3: 1 column X 5cm= $180 \times 5 = 900$

figure 4: 1 column X 5cm= $180 \times 5 = 900$

Figures total = 5040

Equations:  $42 \times 60 = 2520$

No tables

Total character count: 37,540 characters

### Abstract

In many regions of the brain, including the mammalian cortex, the magnitude and direction of activity-dependent changes in synaptic strength depend on the frequency of presynaptic stimulation (synaptic plasticity), as well as the history of activity at those synapses (metaplasticity). We present a model of a molecular mechanism of bidirectional synaptic plasticity based on the observation that long term synaptic potentiation (LTP) and long term synaptic depression (LTD), correlate with the phosphorylation/dephosphorylation of sites on the AMPA receptor subunit protein GluR1. The primary assumption of the model, for which there is wide experimental support, is that the postsynaptic calcium concentration, and consequent activation of calcium-dependent protein kinases and phosphatases, is the trigger for the induction of LTP/LTD. As calcium influx through the NMDA receptor plays a fundamental role in the induction of LTP/LTD, changes in the properties of NMDA receptor calcium influx will dramatically effect activity-dependent synaptic plasticity (metaplasticity). We demonstrate that experimentally observed metaplasticity can be accounted for by activity-dependent regulation of NMDA receptor subunit composition and function. Our model produces a frequency-dependent LTP/LTD curve with a sliding synaptic modification threshold similar to what has been proposed theoretically and has been observed experimentally .

## 1 Introduction

Bidirectional changes in the strength of synaptic responses are fundamental to information storage within neuronal networks. In many regions of the brain, LTP [5], a long-lasting increase in synaptic efficacy, is produced by high frequency stimulation (HFS) of presynaptic afferents or by pairing presynaptic stimulation with robust postsynaptic depolarization [6]. LTD [7], a long-lasting decrease in the strength of synaptic transmission, is produced by low frequency stimulation (LFS) of presynaptic afferents. HFS-induced LTP results in an increase in the amplitude of miniature excitatory postsynaptic currents (mEPSC) and an increase in the response to application of exogenous glutamate [8]. In contrast, LFS-induced LTD results in a decrease in mEPSC amplitude [9, 10] and a decrease in the response to application of exogenous glutamate [11]. Not only are LTP and LTD expressed in many brain regions and in many species, the majority of synapses that express LTP also express LTD. Thus, the regulation of synaptic strength by activity is bidirectional. Such bidirectional regulation of synaptic strength has been hypothesized to depend on changes in the number and/or composition of the AMPA subtype of glutamate receptors (AMPA receptors) in the postsynaptic membrane.

The AMPAR is a heteromer, composed of multiple subtypes of subunit proteins (GluR1-GluR4). AMPAR function is regulated by the composition of individual receptors and/or the phosphorylation/dephosphorylation state of individual subunit proteins. Of particular interest are Serine 831 (S831) and Serine 845 (S845) on the GluR1 subunit, which can be phosphorylated by CaMKII/protein kinase C (PKC) and protein kinase A (PKA) respectively. The induction of LTP specifically increases phosphorylation of S831 [12], which increases, by approximately two fold, the single channel conductance of homomeric GluR1 AMPARs [13]. The induction of LTD is accompanied by a decrease in the phosphorylation of S845, which appears to be phosphorylated at resting potential [14, 15] and phosphorylation of S845 increases the "open time" of the AMPAR [16]. Therefore, knowledge of the phosphorylation state of GluR1 may be a strong predictor of the direction of change (increase or decrease) induced by conditioning stimulation.

In many regions of the brain, including the mammalian cortex, the magnitude and sign of activity-dependent changes in synaptic strength depends on the presynaptic frequency [3], as well as the history of activity at those synapses. We refer to the curve depicting the frequency dependence of changes in synaptic strength as the LTP/LTD curve, and the crossover point between LTD and LTP, the modification threshold. Kirkwood et. al. (1996) have shown that the shape of the LTP/LTD curve, and the value of the modification threshold, depend on the history of cortical activity, which can be acutely regulated *in vivo* by experience or *in vitro* using a stimulation paradigm [4].

Antagonist of NMDA receptors (NMDARs) inhibit the induction of HFS-induced LTP and LFS-induced LTD, suggesting that the NMDAR is the critical point of calcium entry into the postsynaptic neuron. As such, changes in NMDAR function will dramatically alter the properties of activity-dependent synaptic plasticity. NMDARs are heteromeric ion channels, composed of NR1 and NR2 subunit proteins [17, 18]. Each of the four subtypes of the NR2 subunit (2A-2D) confers distinct functional properties to the receptor. As has been demonstrated both *in vivo* and *in heterologous*

expression systems, NMDARs composed of NR1 and NR2B mediate long duration currents ( $\approx 250ms$ ), while inclusion of the NR2A subunit results in NMDARs with faster kinetics ( $\approx 50ms$ ) [19, 20]. NMDARs composed of NR1 and NR2B are observed in the neocortex at birth [19, 20, 21], and over the course of development there is an increase in the ratio of NR2A/NR2B. The composition and function of synaptic NMDARs can also be acutely, and bidirectionally modified by cortical activity [22, 23, 24, 25].

Here we present a model that combines and integrates bidirectional plasticity of AMPAR by calcium dependent phosphorylation and dephosphorylation, (LTP/LTD induction) with plasticity of NMDAR subunit composition. Our model produces a frequency-dependent LTP/LTD curve with a sliding synaptic modification threshold similar to what has been proposed on theoretical grounds [2, 26] and observed experimentally [3, 4].

## 2 Control of synaptic strength by activity-dependent regulation of AMPAR phosphorylation

The bidirectional regulation of phosphorylation of two sites on the GluR1 subunit of the AMPAR, based on the work of Lee, Haganir and Bear, is schematized in figure 1 [14, 27, 15].

The fraction of AMPARs containing GluR1 phosphorylated at S831 is denoted by  $A_{p1}$ , while  $A^{p2}$  denotes the fraction of AMPARs containing GluR1s phosphorylated at S845, and  $A$ , and  $A_{p1}^{p2}$  denote AMPARs phosphorylation at neither and both sites respectively. EP1 and EP2 are used to denote the protein phosphatases which dephosphorylate these two sites, and EK1 and EK2 are used to denote the protein kinases which phosphorylate these sites.

A fundamental assumption of this model, based on experimental data, is that the activity of the protein kinases and protein phosphatases that target these two sites on the GluR1 protein are directly or indirectly regulated by intracellular  $[Ca^{2+}]$  [28, 29].

Thus  $EP1 = EP1(Ca^{2+})$ ,  $EP2 = EP2(Ca^{2+})$ ,  $EK1 = EK1(Ca^{2+})$ ,  $EK2 = EK2(Ca^{2+})$ , where we have used  $Ca^{2+}$ , instead of  $[Ca^{2+}]$  in order to simplify the notation.

The cycle shown in figure 1 can be quantitatively analyzed by two approaches:

a) The Mass Action Law where the enzymes involved are treated as calcium dependent forward and backward rate constants of a reversible reaction:



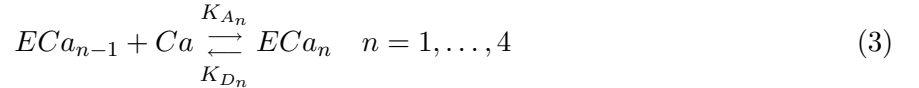
$EK, EP \in \{EK1, EK2, EP1, EP2\}$  is the enzyme kinase or phosphatase;  $A, B \in \{A, A_{p1}, A^{p2}, A_{p1}^{p2}\}$  are the reaction substrates and products.

b) The Michaelis-Menten kinetics for each enzyme of the phosphorylation cycle



where  $E \in \{EK1, EK2, EP1, EP2\}$  is the protein kinase or phosphatase;  $S, P \in \{A, A_{p1}, A^{p2}, A_{p1}^{p2}\}$  are respectively the reactions substrates and products;  $ES$  are the enzyme-substrate complexes,  $k_f, k_b$  are the forward and backward constants,  $k_{irr}$  is the constant for the irreversible step.

We can also consider the  $Ca^{2+}$  dependent activation of each enzyme by the following reaction:



where  $K_{A_n}$  and  $K_{D_n}$  are respectively, the association and the dissociation constant for each reaction,  $ECa_0$  is the bare enzyme and  $ECa_n$  is the fully activated enzyme (bounded with 4  $Ca^{2+}$ ).

These approaches lead to time-evolution equations that can be written in a similar matrix form:

$$\frac{d\mathcal{A}}{dt} = \mathcal{R}_{MA} \cdot \mathcal{A} \quad \frac{d\mathcal{A}}{dt} = \mathcal{R}_{MM} \cdot \mathcal{A} \quad \frac{d\mathcal{A}}{dt} = \mathcal{R}_{MM}^{Ca} \cdot \mathcal{A} \quad (4)$$

where  $\mathcal{A} = (A \quad A_{p1} \quad A^{p2} \quad A_{p1}^{p2})$ ;  $\mathcal{R}_{MA}$ ,  $\mathcal{R}_{MM}$  and  $\mathcal{R}_{MM}^{Ca}$  are the matrices containing the velocities of conversion between the different phosphorylation states of the AMPA receptor calculated by the Mass Action (MA), the Michaelis Menten (MM), and the Michaelis Menten with calcium as activator ( $MM^{Ca}$ ) approach (see Appendix A).

If we assume that the time-course of  $Ca^{2+}$ -dependent activation of each enzyme is faster than the time course of AMPA receptor phosphorylation, we can make the approximation that the enzymatic dynamics are instantaneous. Under such conditions the MA case is exactly solvable (appendix A1) and the stable solutions have the form:

$$\begin{aligned} A &= \frac{A_T \cdot EP1 \cdot EP2}{(EK2 + EP2) \cdot (EK1 + EP1)} & A_{p1} &= \frac{A_T \cdot EK1 \cdot EP2}{(EK2 + EP2) \cdot (EK1 + EP1)} \\ A^{p2} &= \frac{A_T \cdot EP1 \cdot EK2}{(EK2 + EP2) \cdot (EK1 + EP1)} & A_{p1}^{p2} &= \frac{A_T \cdot EK1 \cdot EK2}{(EK2 + EP2) \cdot (EK1 + EP1)}. \end{aligned} \quad (5)$$

Although the MM cases are formally similar, the differential equations that describe their dynamics are not linear. Therefore we do not have an explicit analytical solution for those equations. Nevertheless, they can be solved numerically. In addition we must make assumptions about the calcium dependence of the enzymatic activity. We find two conditions necessary for obtaining the realistic LTP/LTD curves: (1) The activity level of the phosphatases rises at lower calcium concentration than the activity level of the kinases. (2) At high calcium concentrations the activity level of the protein kinases is higher than the activity level of the protein phosphatases. We show that AMPAR conductance depends on the level of intracellular  $Ca^{2+}$ , regardless of the form of  $Ca^{2+}$ -dependent enzymatic activation we apply (sigmoidal, hyperbolic or Hill function).

In figure 2 we show two different sets of assumptions that lead to LTD for a small elevation in calcium levels and LTP for a large elevation. The results in figure 2 are based on the MA model. The AMPAR conductance was calculated by  $conductance = A + 2 * (A_{p1} + A^{p2}) + 4 * A_{p1}^{p2}$ , which

is roughly consistent with experimental results. Using the MM approaches leads to qualitatively similar results (data not shown).

### 3 NMDA receptor calcium influx and plasticity

Calcium influx through NMDA receptors, denoted by  $I_{NMDA}$ , can be broken down into two components, one fast and one slow with time constants  $\tau_f$ ,  $\tau_s$  [22]. We assume that calcium decays passively with a time constant of  $\tau_{Ca}$ , and a voltage dependence as described by Jahr and Stevens (1990) (Appendix B). We can then obtain the average calcium concentration at steady state as :

$$\overline{Ca} = \mathcal{H}(V) \cdot f \cdot \tau_{Ca} (\tau_f N_f + \tau_s N_s) = \mathcal{H}(V) \cdot f \cdot G_{NMDA}. \quad (6)$$

Where  $G_{NMDA}$  is the gain of calcium influx through NMDA receptors,  $V$  is the postsynaptic potential,  $f$  is the presynaptic frequency and  $\mathcal{H}$  describes the voltage dependence of the calcium influx (Appendix B). This implies that the average level of calcium at steady state is linearly related to presynaptic frequency and the magnitude of the fast and slow components ( $N_f$  and  $N_s$ ).

If we assume that synaptic strength depends on the sustained average level of calcium, we can use equation 6 to express AMPAR conductance as a function of presynaptic frequency ( $f$ ) and postsynaptic depolarization ( $V$ ). In figure 3a we show an example of how AMPA conductance depends on these two variables. This figure is based on the MA model described in section 2. It assumes that  $f$  and  $V$  are controlled independently, such as during protocols in which presynaptic stimulation is paired with postsynaptic depolarization [30, 31]. However, in most experimental paradigms, postsynaptic depolarization depends on presynaptic frequency. The diagonal line in figure 3a represents a possible linear dependence of  $V$  on  $f$ . In figure 3b we display the AMPA conductance along this line. This LTP/LTD curve is qualitatively similar to frequency response curves obtained experimentally [7]. This qualitative result is conserved as long as  $V$  monotonically increases with  $f$ .

The composition and function of NMDA receptors changes over the course of development and depends on the history of cortical activity. Changing the kinetics of NMDAR-mediated synaptic currents will effect  $G_{NMDA}$  and will therefore alter the form of the LTP/LTD curve. To account for the activity dependent changes in NMDAR composition and function we develop a phenomenological model for the plasticity of NMDA receptor kinetics. We assume that the total number of NMDA receptors in the membrane is fixed, and that the relative concentration of each type reflects the relative intracellular concentration. This can be expressed by the following set of equations:

$$N_f = \alpha \frac{NR2A}{NR2A + NR2B} \quad N_s = \alpha \frac{NR2B}{NR2A + NR2B} \quad (7)$$

where  $\alpha$  is a proportionality constant. The data indicates that  $NR2A$  levels are activity dependent but levels of  $NR2B$  seem fixed [23]. We therefore assume that  $NR2B$  is constant and that  $NR2A = \langle f(V) \rangle_{\tau_{2A}}$ , where the  $\langle \rangle_{\tau_{2A}}$  represents a temporal average, with a temporal window of

$\tau_{2A}$ . For illustration purposes let us assume that  $NR2A = \langle (V/V_0)^2 \rangle_{\tau_{2A}}$ , where  $V_0$  is an arbitrary proportionality constants. We will then have:

$$G_{\text{NMDA}} = \alpha\tau_{\text{Ca}} \left( \tau_f \frac{\langle (V/V_0)^2 \rangle_{\tau_{2A}}}{\langle (V/V_0)^2 \rangle_{\tau_{2A}} + NR2B} + \tau_s \frac{NR2B}{\langle (V/V_0)^2 \rangle_{\tau_{2A}} + NR2B} \right) \quad (8)$$

The rate of the change depends on  $\tau_{2A}$ <sup>1</sup>, which depends on the time scale for synthesis of new NR2A subunits. The change in  $G_{\text{NMDA}}$  is approximately inversely proportional to the modification threshold.

In figure 4a we illustrate how altering the value of  $G_{\text{NMDA}}$  changes the form of the LTP/LTD curve. This change is qualitatively consistent with experimental results which indicate that the form of the LTP/LTD curve can be altered by changing the level of cortical activity [3, 4]. For comparison we replotted the results of Kirkwood et. al. (1996) in figure 4b. The activity dependence of the LTP/LTD curve as described by equation 8 and illustrated in figure 4 is consistent with a key postulate of the BCM theory; the sliding modification threshold.

## 4 Discussion

We present a model of the molecular mechanism of synaptic plasticity which implies that knowing the local postsynaptic concentration of intracellular calcium is sufficient to determine the status of AMPAR subunit phosphorylation, and therefore, synaptic efficacy. The fundamental assumption of the model is that the intracellular calcium concentration is the principal trigger for the induction of LTD/LTP, an assumption that has wide experimental support. One of the principal features of this model is its relative robustness to the detailed assumptions; the same qualitative form of an LTP/LTD curve is obtained assuming different functional forms for the calcium dependence of the enzymes and when using different mathematical formalisms.

By using a known model of NMDAR calcium conductance, and by taking a temporal average of the calcium concentration, we can convert the model to a form that depends on postsynaptic voltage and presynaptic frequency (figure 3a) or to a model that depends only on presynaptic frequency (figure 3b). We have also demonstrated that a phenomenological model for the modification of NMDAR subunit composition can account for the sliding modification threshold [2, 3, 4].

This mathematical model provides a link between synaptic plasticity observed in situ, and biochemical/electrophysiological observations of glutamate receptor composition and function. Further, it combines plasticity of AMPA and NMDA receptors. A consequence of the proposed mechanism of the sliding modification threshold is that for animals raised in deprived conditions the minima of the LTP/LTD curve should occur at lower frequencies than for normally reared animals, and this

---

<sup>1</sup>Note that  $\tau_f$  the decay time constant of the NMDA heteromers with the NR2A subunit and  $\tau_{2A}$  are different variables

minima should be of equivalent magnitude (figure 4a). Although there already is experimental evidence for a sliding modification threshold, further experiments that would measure the magnitude of these minima would test our theoretical framework.

The biophysical model supports the postulates of the BCM theory [2, 26, 32], but, as expected, suggest detailed modifications. For example, the BCM theory is formulated in terms of the temporal derivative of the synaptic weight. Here, we extract a rule directly for the fixed point of the synaptic weights, for given presynaptic frequency and postsynaptic potential. Under certain conditions these can be related by the addition of a weight decay term (Shouval et. al. in preparation). In addition, to attain stability, the synaptic modification threshold of the BCM theory was chosen to be a super-linear function of activity. In our model we obtain a functional form that is more complex, and the dynamic range of the modification threshold is finite. The effect of these differences on the stability of learning, on the formation of receptive fields and on the ability to account for various experimental results are currently being studied. Further, we are currently examining how this framework could account for more transient induction mechanisms such a spike time dependent plasticity [33, 34].

## References

- [1] W. C. Abraham and Mark F. Bear. Metaplasticity: the plasticity of synaptic plasticity. *Trends Neurosci.*, 19(4):126–30, 1996.
- [2] E. L. Bienenstock, L. N Cooper, and P. W. Munro. Theory for the development of neuron selectivity: orientation specificity and binocular interaction in visual cortex. *Journal of Neuroscience*, 2:32–48, 1982.
- [3] A. Kirkwood, M. G. Rioult, and M. F. Bear. Experience-dependent modification of synaptic plasticity in visual cortex. *Nature*, 381:526–528, 1996.
- [4] Hongyan Wang and John J. Wagner. Priming-induced shift in synaptic plasticity in the rat hippocampus. *Journal of Neurophysiology*, 82(4):2024–2028, 1999.
- [5] T. V. P. Bliss and T. Lømo. Long-lasting potentiation of synaptic transmission in the dentate area of the anesthetized rabbit following stimulation of the perforant path. *J. Physiol. , London*, 232, 1973.
- [6] H Wigstrom and B. Gustafsson. Postsynaptic control of hippocampal long-term potentiation. *J Physiol (Paris)*, 81:228–36, 1986.
- [7] S. M. Dudek and M. F. Bear. Homosynaptic long-term depression in area CA1 of hippocampus and the effects on NMDA receptor blockade. *Proc. Natl. Acad. Sci.*, 89:4363–4367, 1992.
- [8] S N Davies, R A Lester, K G Reymann, and G L Collingridge. Temporally distinct pre- and post-synaptic mechanisms maintain long-term potentiation. *Nature*, 338:500–3, 1989.
- [9] S H Oliek, R. C. Malenka RC, and R. A. Nicoll. Bidirectional control of quantal size by synaptic activity in the hippocampus. *Science*, 271:1294–7, 1996.
- [10] R C Carroll, D V Lissin, M von Zastrow, R A Nicoll, and R C Malenka. Rapid redistribution of glutamate receptors contributes to long-term depression in hippocampal cultures. *Nat Neurosci*, 2:454–60, 1999.

- [11] K. Kandler, L C Katz, and J A Kauer. Focal photolysis of caged glutamate produces long-term depression of hippocampal glutamate receptors. *Nat Neurosci*, 1:119–23, 1998.
- [12] A. Barria, D. Muller, V. Derkach, and T. R. Soderling. Regulatory phosphorylation of ampa-type glutamate receptors by CaM-KII during long term potentiation. *Science*, 276:2042–2045, 1997.
- [13] V. Derkach, A. Barria A, and TR Soderling. Ca<sup>2+</sup>/calmodulin-kinase II enhances channel conductance of alpha-amino-3-hydroxy-5-methyl-4-isoxazolepropionate type glutamate receptors. *Proc Natl Acad Sci.*, 96(6):3269–74, 1999.
- [14] H-K Lee, K. Kameyama, R.L. Huganir, and M.F. Bear. NMDA induces long-term synaptic depression and dephosphorylation of the GluR1 subunit of AMPA receptors in hippocampus. *Neuron*, 21(5):1151–62, 1998.
- [15] H-K Lee, M. Barbarosie, K. Kameyama, M. F. Bear, and R. L. Huganir. Regulation of distinct AMPA receptor phosphorylation sites during bidirectional synaptic plasticity. *Nature*, 405:955–9, 2000.
- [16] T. G. Banke, D. Bowie<sup>1</sup>, H.-K. Lee, R. L. Huganir, A. Schousboe, and S. F. Traynelis. Control of GluR1 AMPA receptor function by cAMP-Dependent protein kinase. *Journal of Neuroscience*, 20(1):89–102, 2000.
- [17] C. J. McBain and M. L. Mayer. N-methyl-D-aspartic acid receptor structure and function. *Physiol Rev*, 74:723–760, 1994.
- [18] R S Zukin and M V Bennett. Alternatively spliced isoforms of the NMDAR receptor subunit. *Trends Neurosci.*, 18:306–13, 1995.
- [19] G Stocca and S Vicini. Increased contribution of NR2A subunit to synaptic nmda receptors in developing rat cortical neurons. *J Physiol*, 507:13–24, 1998.
- [20] A C Flint, U S Maisch, J H Weishaupt, A R Kriegstein, and H Monyer. NR2A subunit expression shortens nmda receptor synaptic currents in developing neocortex. *J Neurosci.*, 17:2469–76, 1997.
- [21] M Sheng, J. Cummings, L. A. Roldan, Y. N. Jan, and L. Y. Jan. Changing subunit composition of heteromeric NMDA receptors during development of rat cortex. *Nature*, 368:144–147, 1994.
- [22] G. Carmignoto and S. Vicini. Activity dependent increase in NMDA receptor responses during development of visual cotex. *Science*, 258:1007–1011, 1992.
- [23] Elizabeth M. Quinlan, B.D. Philpot, R.L. Huganir, and M.F. Bear. Rapid, experience-dependent expression of synaptic NMDA receptors in visual cortex in vivo. *Nature Neuroscience*, 2(4):352–357, 1999.
- [24] Elizabeth M. Quinlan, Daniel H. Olstein, and Mark F. Bear. Bidirectional, experience-dependent regulation of nmda receptor subunit composition in rat visual cortex during postnatal development. *Proceedings of the National Academy of Science*, 96:1287–1290, 1999.
- [25] Benjamin D. Philpot, Aarti K. Sekhar, Harel Z. Shouval, and Mark F. Bear. Visual experience and deprivation bidirectionally modify the composition and function of NMDA receptors in visual cortex. *Neuron*, 29:157–69, 2001.
- [26] N. Intrator and L. N Cooper. Objective function formulation of the BCM theory of visual cortical plasticity: Statistical connections, stability conditions. *Neural Networks*, 5:3–17, 1992.

- [27] Kimihiko Kameyama, H-K. Lee, M.F. Bear, and R. L. Huganir. Involvement of a postsynaptic protein kinase a substrate in the expression of homosynaptic long-term depression. *Neuron*, 21(5):1163–75, 1998.
- [28] J. A. Lisman. A mechanism for the Hebb and the anti-Hebb processes underlying learning and memory. *Proceedings of the National Academy of Science*, 86:9574–9578, 1989.
- [29] Tobias Meyer, Phyllis I. Hanson, Lubert Stryer, and Howard Shulman. Calmodulin trapping by calcium-calmodulin dependent protein kinase. *Science*, pages 1199–1201, 1992.
- [30] M. C. Crair and R. C. Malenka. A critical period for long-term potentiation at thalamocortical synapses. *Nature*, 375:325–8, 1995.
- [31] Dan E. Feldman, Roger A. Nicoll, Robert C. Malenka, and J. T. Isaac. Long-term depression at thalamocortical synapses in developing rat somatosensory cortex. *Neuron*, 21(2)::347–57, 1998.
- [32] Brian Blais, Harel Shouval, and Leon N Cooper. The role of presynaptic activity in monocular deprivation: Comparison of homosynaptic and heterosynaptic mechanisms. *Proc. Natl. Acad. Sci.*, 96:1083–1087, 1999.
- [33] H. Markram, J. Lübke, M. Frotscher, and B. Sakmann. Regulation of synaptic efficacy by coincidence of postsynaptic APs and EPSPs. *Science*, 275:213–215, 1997.
- [34] G. Bi and M. Poo. Synaptic modifications in cultured hippocampal neurons: Dependence on spike timing, synaptic strength, and postsynaptic cell type. *The Journal of Neuroscience*, 18 (24):10464–10472, 1998.
- [35] C. E. Jahr and C. F. Stevens. Voltage dependence of nmda-activated macroscopic conductances predicted by single-channel kinetics. *J. Neurosci.*, 10:3178–82, 1990.
- [36] Daniel Johnston and Samuel M. S. Wu. *Foundations of Cellular Neurophysiology*. MIT press, Cambridge, MA, 1995.

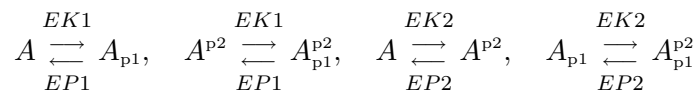
## Acknowledgments

This research was supported by The Charles A. Dana Foundation, GCC was supported by an exchange program between Bologna and Brown University and MURST (60%). We would also wish to thank Mark Bear, Hey-Kyoung Lee and Irina Vayl for useful discussions.

## A AMPAR phosphorylation cycle dynamics

### A.1 Mass Action Approach

By applying the Mass Action Law to the phosphorylation cycle showed in Fig 1, which assumes two phosphorylation sites, we observe that it is composed by four reversible reactions:



and it is easy to obtain the following time-evolution system:

$$\begin{pmatrix} \dot{A} \\ \dot{A}_{p1} \\ \dot{A}^{p2} \\ \dot{A}_{p1}^{p2} \end{pmatrix} = \begin{pmatrix} -(EK1 + EK2) & EP1 & EP2 & 0 \\ EK1 & -(EP1 + EK2) & 0 & EP2 \\ EK2 & 0 & -(EP2 + EK1) & EP1 \\ 0 & EK2 & EK1 & -(EP1 + EP2) \end{pmatrix} \begin{pmatrix} A \\ A_{p1} \\ A^{p2} \\ A_{p1}^{p2} \end{pmatrix} \quad (9)$$

The system (9) can be rewritten as  $\dot{\mathcal{A}} = \mathcal{R}_{MA} \cdot \mathcal{A}$  where  $\mathcal{A} = (A, A_{p1}, A^{p2}, A_{p1}^{p2})$  and  $\mathcal{R}_{MA}$  is the "coefficients matrix". In order to characterize the equilibrium solution we observe that the kernel of the matrix  $\mathcal{R}_{MA}$  is, by construction, not trivial ( $Det(\mathcal{R}_{MA}) = 0$ ) and one of its basis is:

$$\vec{B}_{Ker(\mathcal{R}_{MA})} = \left( \frac{\mathcal{M}_1}{\mathcal{M}_4} \quad \frac{\mathcal{M}_2}{\mathcal{M}_4} \quad \frac{\mathcal{M}_3}{\mathcal{M}_4} \quad 1 \right) \quad (10)$$

where

$$\mathcal{M}_1 = P1 \cdot P2 \cdot P2 + K1 \cdot P2 \cdot P1 + P1 \cdot P2 \cdot K1 + K2 \cdot P2 \cdot P1, \quad \mathcal{M}_2 = K1 \cdot P2 \cdot P2 + K1 \cdot P2 \cdot K1 + K1 \cdot P1 \cdot P1 + P2 \cdot K2 \cdot K1$$

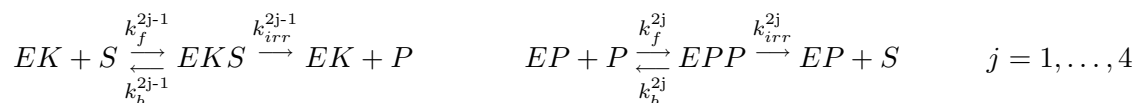
$$\mathcal{M}_3 = K2 \cdot K2 \cdot P1 + P1 \cdot K2 \cdot P1 + P1 \cdot P2 \cdot K2 + K1 \cdot K2 \cdot P1, \quad \mathcal{M}_4 = K1 \cdot K2 \cdot K1 + K2 \cdot K2 \cdot K1 + K1 \cdot K2 \cdot P2 + P1 \cdot K2 \cdot K1.$$

Now, the conservation of the total amount of AMPAr ( $A(t) + A_{p1}(t) + A_{p2}(t) + A_{p1}^{p2}(t) = A_T$ ) leads to the following equilibrium solutions as fractions of  $A_T$ :

$$\mathcal{A}_\infty = \left( \frac{\mathcal{M}_1 \cdot A_T}{\sum_{i=1}^4 \mathcal{M}_i}, \frac{\mathcal{M}_2 \cdot A_T}{\sum_{i=1}^4 \mathcal{M}_i}, \frac{\mathcal{M}_3 \cdot A_T}{\sum_{i=1}^4 \mathcal{M}_i}, \frac{\mathcal{M}_4 \cdot A_T}{\sum_{i=1}^4 \mathcal{M}_i} \right) \quad (11)$$

## A.2 Michealis Menten Approach

The AMPAr cycle showed in Fig 1 is composed by four coupled enzymatic reactions, one phosphorylation and one dephosphorylation:



where  $EK, EP \in \{EK1, EK2, EP1, EP2\}$ ;  $S, P \in \{A, A_{p1}, A^{p2}, A_{p1}^{p2}\}$ . The constant  $k_f^i, k_b^i, k_{irr}^i$   $i = 1, \dots, 8$  are the rate constants for the forward, backward and irreversible step. According to the Michaelis Menten analysis we define the Michaelis Menten constants  $k_m^i = \frac{k_b^i + k_{irr}^i}{k_f^i}$   $i = 1, \dots, 8$ . The application of the Pseudo Steady State hypothesis as well the Mass Action Law allows us to write the following time-evolution system for the concentrations of the different fractions of AMPAr for each phosphorylation state:

$$\dot{\mathcal{A}} = \mathcal{R}_{MM} \cdot \mathcal{A}; \quad (12)$$

where  $\mathcal{A} = (A, A_{p1}, A^{p2}, A_{p1}^{p2})$ , and  $\mathcal{R}_{MM}$  is a "coefficient matrix" :

$$\mathcal{R}_{MM} = \begin{pmatrix} -(c_1\mathcal{F}_{EK1} + c_2\mathcal{F}_{EK2}) & c_3\mathcal{F}_{EP1} & c_4\mathcal{F}_{EP2} & 0 \\ c_1\mathcal{F}_{EK1} & -(c_5\mathcal{F}_{EK2} + c_3\mathcal{F}_{EP1}) & 0 & c_6\mathcal{F}_{EP2} \\ c_2\mathcal{F}_{EK2} & 0 & -(c_7\mathcal{F}_{EK1} + c_4\mathcal{F}_{EP2}) & c_8\mathcal{F}_{EP1} \\ 0 & c_5\mathcal{F}_{EK2} & c_7\mathcal{F}_{EK1} & -(c_8\mathcal{F}_{EP1} + c_6\mathcal{F}_{EP2}) \end{pmatrix} \quad (13)$$

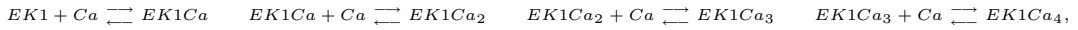
Where:

$$\begin{aligned} c_1 &= k_{irr}^1 \cdot k_m^7, & c_2 &= k_{irr}^5 \cdot k_m^3, & c_3 &= k_{irr}^2 \cdot k_m^8, & c_4 &= k_{irr}^6 \cdot k_m^4, \\ c_5 &= k_{irr}^3 \cdot k_m^5, & c_6 &= k_{irr}^4 \cdot k_m^6, & c_7 &= k_{irr}^7 \cdot k_m^1, & c_8 &= k_{irr}^8 \cdot k_m^2 \end{aligned}$$

and the four “fluxes” have the form:

$$\begin{aligned} \mathcal{F}_{EK1} &= \frac{EK1_T}{k_{m1}k_{m7} + k_{m1}A^{p2} + k_{m7}A} & ; & & \mathcal{F}_{EP1} &= \frac{EP1_T}{k_{m2}k_{m8} + k_{m2}A_{p1}^{p2} + k_{m8}A_{p1}} \\ \mathcal{F}_{EK2} &= \frac{EK2_T}{k_{m3}k_{m5} + k_{m3}A + k_{m5}A_{p1}} & ; & & \mathcal{F}_{EP2} &= \frac{EP2_T}{k_{m4}k_{m6} + k_{m4}A^{p2} + k_{m6}A_{p1}^{p2}}, \end{aligned}$$

where  $EK1_T, EP1_T, EK2_T, EP2_T$  are the total amounts of each enzymes. Note that equation (12) has a form that is similar to the one written down for the reversible reaction ( we can characterize  $Ker(\mathcal{R}_{MM})$ ), however there is a significant difference since the “fluxes” are functions of the dynamic variables, not constants. Thus this equation is non linear and a full solution of the dynamics has not been analytically obtained. Previous derivations have assumed that the levels of the enzymes’ activity depends on calcium levels, we made ad hoc assumptions about this dependence. The calcium dependence of these enzymes can be calculated if we know how calcium interacts with them, for example EK1, needs to be bound to calcium in order to switch an active state ( $Ca^{2+}$  is an activator for EK1). More generally, and according to various experimental findings, we can assume that each enzyme needs to be bound to more than one molecule of Calcium. Here we will assume that activation depends on calcium binding at four sites, thus we have the following reaction sequence:



with the association constant  $K_I, K_{II}, K_{III}, K_{IV}$  for each binding site. With these assumptions, we can write the “fluxes” for the AMPAr cycle with four enzymes (see Web supplement):

$$\begin{aligned} \mathcal{F}_{EK1}^{Ca} &= \frac{EK1_T \cdot \sigma_{EK1}(Ca)}{k_m^1 k_m^7 + k_m^1 \cdot \sigma_{EK1}(Ca)A^{p2} + k_m^7 \cdot \sigma_{EK1}(Ca)A} & ; & & \mathcal{F}_{EP1}^{Ca} &= \frac{EP1_T \sigma_{EP1}(Ca)}{k_m^2 k_m^8 + k_m^2 \sigma_{EP1}(Ca)A_{p1}^{p2} + k_m^8 \sigma_{EP1}(Ca)A_{p1}} \\ \mathcal{F}_{EK2}^{Ca} &= \frac{EK2_T \sigma_{EK2}(Ca)}{k_m^3 k_m^5 + k_m^3 \sigma_{EK2}(Ca)A + k_m^5 \sigma_{EK2}(Ca)A_{p1}} & ; & & \mathcal{F}_{EP2}^{Ca} &= \frac{EP2_T \sigma_{EP2}(Ca)}{k_m^4 k_m^6 + k_m^4 \sigma_{EP2}(Ca)A^{p2} + k_m^6 \sigma_{EP2}(Ca)A_{p1}^{p2}}. \end{aligned}$$

Where the  $\sigma_i$   $i \in (EK1, EK2, EP1, EP2)$  are the functions for the calcium bound of each enzyme:

$$\sigma_i = \frac{(Ca)^4}{K_{I_j} K_{II_j} K_{III_j} K_{IV_j} + K_{II_j} K_{III_j} K_{IV_j} \cdot Ca + K_{III_j} K_{IV_j} \cdot (Ca)^2 + K_{IV_j} \cdot (Ca)^3 + (Ca)^4}; \quad i = j \in \{EK1, EK2, EP1, EP2\}$$

With this formalism we can write again the system as  $\dot{A} = \mathcal{R}_{MM}^{Ca} \cdot A$  where the matrix  $\mathcal{R}_{MM}^{Ca}$  is obtained by substitution of the fluxes  $\mathcal{F}_j$  with the calcium dependent fluxes  $\mathcal{F}_j^{Ca}$ . So also in this case we can characterize  $Ker(\mathcal{R}_{MM}^{Ca})$  and numerically solve the system.

## B Calcium dynamics through NMDA channels

A simple differential equation that qualitatively captures the main features of the calcium dynamics in spines is

$$\frac{d[Ca(t)]}{dt} = I_{NMDA}(t) - \frac{1}{\tau_{Ca}}[Ca(t)] \quad (14)$$

where  $[Ca(t)]$  is the calcium concentration at the spine at time  $t$ ,  $\tau_{Ca}$  is the decay time constant of calcium in the spine. This equation can be solved exactly to yield the solution

$$[Ca(t)] = e^{-\frac{t}{\tau_{Ca}}} \left[ \int_0^t e^{\frac{t'}{\tau_{Ca}}} I_{NMDA}(t') dt' \right]. \quad (15)$$

Given the NMDA current we can calculate the instantaneous level of calcium.

We now assume  $I_{NMDA}(t)$  has the following form:

$$I_{NMDA}(t) = \sum_{\{t_i\}} \left[ N_f \theta(t_i) e^{-\frac{-(t-t_i)}{\tau_f}} + N_s \theta(t_i) e^{-\frac{-(t-t_i)}{\tau_s}} \right] \mathcal{H}(V), \quad (16)$$

where  $t_i$  are the times at which presynaptic spikes are delivered and  $\theta(t)$  is zero for  $t < 0$  and one for  $t > 0$ . The calcium current through NMDA receptors is assumed to have a fast and a slow component with time constants  $\tau_f$  and  $\tau_s$  respectively and magnitudes  $N_f$  and  $N_s$ . The voltage dependence of the calcium current through the NMDA receptors is summarized by  $\mathcal{H}$ . Where  $\mathcal{H}(V)$  expresses the voltage dependence of the calcium current through the NMDA receptors. This depends on the voltage dependence of the magnesium block and on the voltage dependent driving force. Thus we use  $\mathcal{H}(V) = B(V)(V - V_r)$ , where  $B$  represents the dependence on the magnesium block and  $(V - V_r)$  is the driving force for calcium molecules. For  $B$  we use a model based on experimental results [35] which give the functional form of effect of the magnesium block as:

$$B(V) = \frac{1}{(1 + e^{-(0.062 \cdot V)})(Mg/3.57)},$$

where  $Mg$  is the extra-cellular magnesium concentration, in all the subsequent results we assume that  $Mg = 1mM$ . The linear model for the voltage dependence of the driving force is not exact for calcium channels [36] however it is sufficient for our purposes. We also assume a calcium reversal potential of  $130mV$ .

By substituting equation 16 into equation 15 and carrying out the integration we obtain:

$$[Ca(t)] = \mathcal{H}(V) \sum_{\{t_i\}} \left\{ N_f \frac{\tau_f \tau_{Ca}}{\tau_f - \tau_{Ca}} \left[ e^{-\frac{-(t-t_i)}{\tau_f}} - e^{-\frac{-(t-t_i)}{\tau_{Ca}}} \right] + N_s \frac{\tau_s \tau_{Ca}}{\tau_s - \tau_{Ca}} \left[ e^{-\frac{-(t-t_i)}{\tau_s}} - e^{-\frac{-(t-t_i)}{\tau_{Ca}}} \right] \right\} \quad (17)$$

This result is valid based on the assumption that the postsynaptic potential  $V$  is constant which enables us to take this out of the integral. If we stimulate the synapse with a steady frequency  $f$  then the period between two consecutive presynaptic spikes is  $T = 1/f$  and  $t_i = i/f$ , where  $i = 0 \dots N$  and  $N \cdot f < t$ . We can then redefine  $t = N/f + \Delta t$  where  $\Delta t$  is the time since the last presynaptic spike. Thus  $t - t_i = \Delta t + m/f$  where  $m = 0, \dots, N$ . We then have that

$$Ca(t) = Ca(\Delta t, N) = \mathcal{H}(V) \sum_{j=0}^{N-1} \left\{ N_f \frac{\tau_f \tau_{Ca}}{\tau_f - \tau_{Ca}} \left[ e^{\frac{-\Delta t}{\tau_f}} e^{\frac{-j}{f\tau_f}} - e^{\frac{-\Delta t}{\tau_{Ca}}} e^{\frac{-j}{f\tau_{Ca}}} \right] + N_s \frac{\tau_s \tau_{Ca}}{\tau_s - \tau_{Ca}} \left[ e^{\frac{-\Delta t}{\tau_s}} e^{\frac{-j}{f\tau_s}} - e^{\frac{-\Delta t}{\tau_{Ca}}} e^{\frac{-j}{f\tau_{Ca}}} \right] \right\}$$

This result could be expected from the single spike result since it is a solution of a linear differential equation. Now we will concentrate on the steady state solution on the Calcium current, mathematically this implies that  $N \rightarrow \infty$ . The steady state solution exists if the infinite series converges. In the infinite series above we have terms of the form  $\sum_{j=0}^{\infty} e^{\frac{-j}{f\tau_f}} = \frac{1}{1 - e^{-1/f\tau_f}} = \mu_f$ . This series converges since  $e^{\frac{-1}{f\tau_f}} < 1$ .

Thus

$$Ca(\Delta t) = N_f \frac{\tau_f \tau_{Ca}}{\tau_f - \tau_{Ca}} \left( \mu_f e^{\frac{-\Delta t}{f\tau_f}} - \mu_{Ca} e^{\frac{-\Delta t}{f\tau_{Ca}}} \right) + N_s \frac{\tau_s \tau_{Ca}}{\tau_s - \tau_{Ca}} \left( \mu_s e^{\frac{-\Delta t}{f\tau_s}} - \mu_{Ca} e^{\frac{-\Delta t}{f\tau_{Ca}}} \right). \quad (18)$$

Notice that this steady state solution is periodic with periodicity  $T = 1/f$ . We will now calculate the average calcium concentration at steady state by averaging over a period, thus

$$\overline{Ca} = \frac{1}{T} \int_0^T Ca(\Delta t) d(\Delta t) = \mathcal{H}(V) f \tau_{Ca} (\tau_f N_f + \tau_s N_s) = \mathcal{H}(V) f \cdot G_{NMDA}. \quad (19)$$

where  $G_{NMDA} = \tau_{Ca} (\tau_f N_f + \tau_s N_s)$  is the gain of the NMDAr calcium conductance.

This result implies that the average level of calcium at steady state is linearly dependent on presynaptic frequency and that its dependence on the magnitude of the fast and slow components ( $N_f$  and  $N_s$ ) is also simply linear. Equation 19 can now be used to rewrite the equations describing AMPA receptor plasticity in terms of frequency ( $f$ ) and postsynaptic depolarization ( $V$ ), variables that are more readily controlled than intracellular calcium concentration. In order to do this we need to we have to know how calcium concentrations depend on both the presynaptic activity and the postsynaptic depolarization.

## Figure Captions

### Figure 1

An idealized model for the cycle of GluR1 phosphorylation/dephosphorylation at two sites. The model assumes 2 specific kinases (**EK1,EK2**) and two opposing specific phosphatases (**EP1,EP2**). It is assumed that HFS preferentially stimulates the activity of protein kinases, resulting in GluR1 phosphorylation, while LFS preferentially stimulates the activity of protein phosphatases, resulting in GluR1 dephosphorylation.

### Figure 2

Robustness of results of the mass-action approach to  $Ca^{2+}$ -dependent enzymatic reactions, that regulate GluR1 phosphorylation and AMPAR conductance. **(a)** The kinase-phosphatase activity is assumed to be a Hill function of  $Ca$ , with exponent 2.  $EP1(Ca) = EP2(Ca) = 1 + 30 \frac{(Ca)^2}{1+(Ca)^2}$  and  $EK1(Ca) = EK2(Ca) = 1 + 100 \frac{(Ca)^2}{8^2+(Ca)^2}$ . **(b)** Phosphorylation of GluR1 as a function of  $Ca^{2+}$ , using the enzymatic activity assumed in **a**. **(c)** Conductance of AMPAR (in arbitrary units) as a function of calcium. At moderate calcium levels LTD is attained whereas at higher calcium levels LTP is induced. **(d)** The kinase-phosphatase activity of each enzyme in which a sigmoidal dependence on  $Ca$  is assumed:  $EP1 = 10 \frac{30}{10+20 \cdot e^{-(2 \cdot Ca)}}$ ,  $EP2 = 10 \frac{20}{10+10 \cdot e^{-(2.5 \cdot Ca)}}$ ,  $EK1 = 10 \frac{100}{10+90 \cdot e^{-(0.2 \cdot Ca)}}$ ,  $EK2 = 10 \frac{80}{10+70 \cdot e^{-(0.25 \cdot Ca)}}$ . **(e)** Phosphorylation of GluR1 as a function of  $Ca^{2+}$ , using the enzymatic activity assumed in **d**. **(f)** Conductance of AMPAR (in arbitrary units) as a function of calcium.

### Figure 3

Synaptic strength, measured as AMPAR conductance depicted as a function of presynaptic stimulation frequency ( $f$ ) and postsynaptic membrane voltage ( $V$ ). **(a)** A two-dimensional plot depicting postsynaptic membrane potential as a function of presynaptic stimulation frequency. The grey scale indicates the conductance level of the AMPAR. At low stimulation frequencies and postsynaptic voltages the conductance is below baseline, defined as  $f = 0$ ,  $V = -100$ . The diagonal line indicates a linear  $f - V$  relation, which we assume to extract the results in **b**. **(b)** AMPAR conductance as a function of presynaptic stimulation frequency, where a linear dependence of  $V$  on  $f$  is assumed (as shown in **a**). Low frequency stimulation induces LTD whereas high frequency stimulation induces LTP.

Figure 4

The effect of changing NMDA subunit composition on the shape of the LTP/LTD curve. **(a)** We use here the same approach as in figure 3 to produce an LTP/LTD curve as a function of frequency. The two curves reflect two different conductance levels  $G_{\text{NMDA}} = 0.01$  and  $G_{\text{NMDA}} = 0.03$ . NMDA conductance level could change as a function of NMDA subunit composition. We used a semi-log plot to facilitate comparison to experimental results. **(b)** Results reproduced from Kirkwood et. al. (1996) in which LTP/LTD curves of light-reared and dark-reared animals are compared. Notice that these two sets of results are qualitatively consistent.

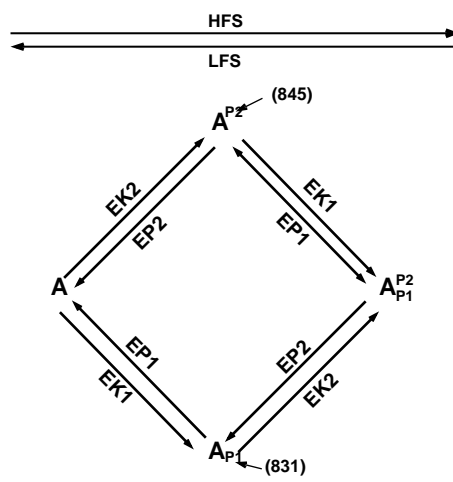


Figure 1:

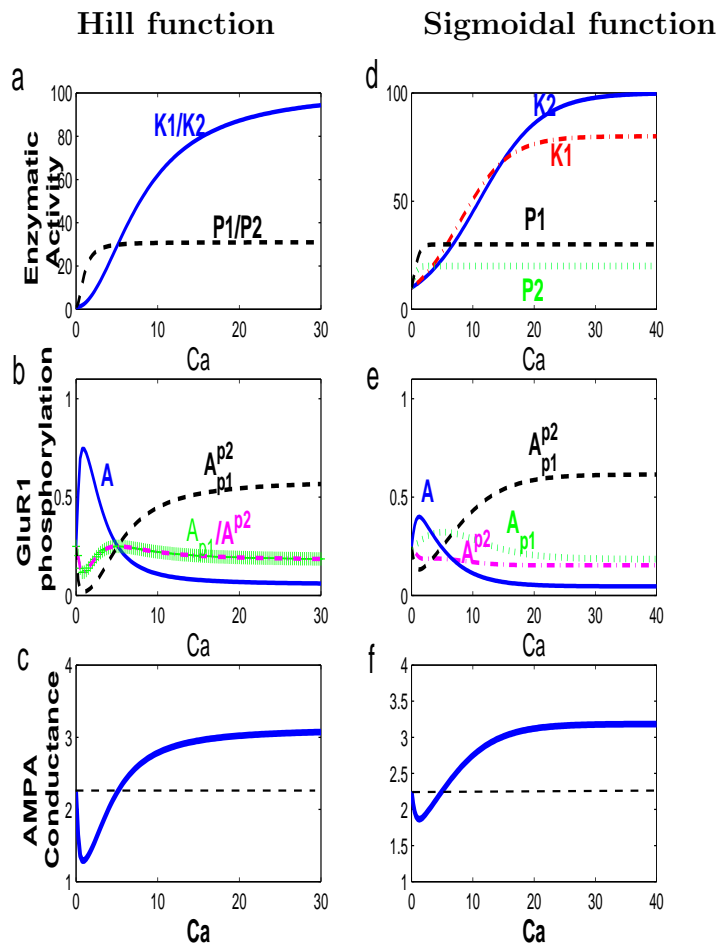


Figure 2:

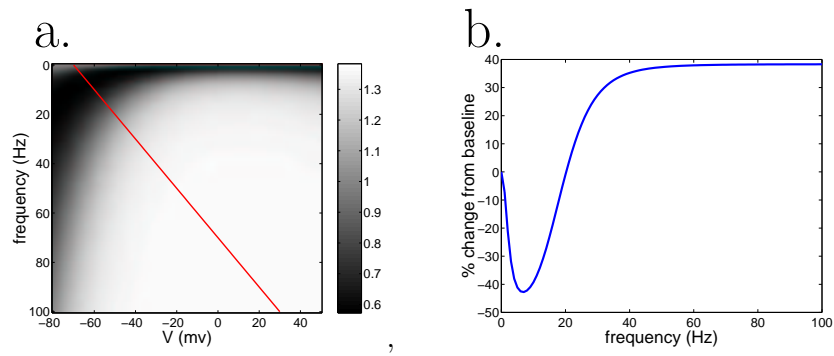


Figure 3:

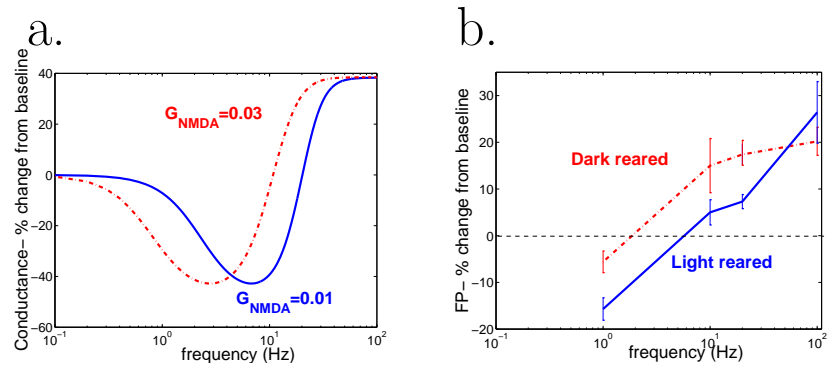


Figure 4: